Pramana – J. Phys. (2019) 92:94
https://doi.org/10.1007/s12043-019-1753-z

Solitary wave and modulational instability in a strongly coupled semiclassical relativistic dusty pair plasma with density gradient

SHATADRU CHAUDHURI[1], K ROY CHOWDHURY[1] and A ROY CHOWDHURY[2,*]

[1]Department of Physics, Jadavpur University, 188, Raja S.C. Mallick Road, Kolkata 700032, India
[2]Department of Physics, High Energy Physics Division, Jadavpur University, 188, Raja S.C. Mallick Road, Kolkata 700032, India
*Corresponding author. E-mail: arc.roy@gmail.com

MS received 24 January 2018; revised 26 October 2018; accepted 20 November 2018;
published online 8 April 2019

Abstract. Using a set of fluid equations to describe the inertial dust grain component in a dense collisionless unmagnetised plasma under the influence of weakly relativistic semiclassical electrons and positrons, the propagation of dust-acoustic wave is studied in the strong coupling regime when the dust density is non-uniform. Our main aim is to analyse the role of semiclassical and relativistic environment (frequently encountered in astrophysical context) on various features of strongly coupled dusty plasma. The semiclassical environment of the electrons and positrons is assumed to be described by the Chandrasekhar equation of state. Our second aim is to see the effect of spatial variation of the dust equilibrium density, which is known to occur due to the deformation of the Debye sheath which in turn leads to polarisation force. A new type of nonlinear Schrödinger equation with spatially varying coefficient is deduced and its modulational stability is studied in detail. In the last section, we have taken recourse to Madelung picture to deduce a variable coefficient Korteweg–de Vries equation from this new nonlinear Schrödinger equation.

Keywords. Density gradient plasma; stellar plasma; dusty plasma; strongly coupled plasma.

PACS Nos **52.35.–g; 52.27.Lw; 52.27.Ep; 95.30.Qd**

1. Introduction

A dusty plasma is characterised by the presence of massive charged dust grains in addition to the electron–ion and neutral particles. They are of various sizes, from nanometres to millimetres. This has become a very important domain of research due to its application in astrophysics, semiconductors, fusion reactors and so on. The dust-acoustic waves (DAWs) [1,2] have been observed in many low-temperature laboratory experiments. This has made it an important area of research in astrophysical environments such as the interior of white dwarfs, which are composed of electrons and positrons in coexistence with a small fraction of ions. As energy is gradually lost, matter cools down, and the particles may behave in a quasiclassical manner although still in a quantum environment. Another important aspect of the present day plasma research is its strong coupling of dust particles, which has been seen to give rise to many new features in DAW propagation. One of the foremost formulation of strongly coupled plasma was that of Gozadinos *et al* [3], where the concept of electrostatic pressure was introduced. It has been applied to the DAW mode [4] and nonlinear solitary wave structure [5,6]. Many of these analyses were about the properties of the DAW mode in quantum plasma due to the importance of quantum effect in space environments and dense astrophysical plasma [7–9]. A very interesting event in plasma physics is that dust grains may experience significant electrostatic forces from their neighbours. It was Ikezi [10] who first predicted that a dusty plasma can enter a strongly coupled regime due to the high charge and low temperature, which makes the coupling $\Gamma = z_{\mathrm{d}}^2 e^2/4\pi\varepsilon_0 k_{\mathrm{B}} T_{\mathrm{d}} a_{\mathrm{d}} \gg 1$. At this point, it may be added that there is more than one approach to the formulation of a strongly coupled plasma. One is the viscoelastic theory followed by Veeresha *et al* [11]. They actually started from the generalised hydrodynamic equations that modify the momentum equation using the integro-differential term,

containing the viscoelastic function characterised by the viscosity term and relaxation time. Collective oscillations in weakly coupled dusty plasmas, such as DA and DIA modes, have been extensively studied theoretically [12,13] and experimentally [14]. But a very significant aspect that has been overlooked is the inhomogeneity or density gradient. The effect of density gradient on the role played by strongly coupled plasma is not yet fully understood. Spatial inhomogeneous equilibrium density may occur in a dusty plasma due to the distribution of immobile dust grains [15,16]. For a strongly coupled plasma that is still in a fluid state, coupling of shear and compressional modes occurs that can also lead to spatial variation. Such variation of equilibrium density is responsible for many important events. For example, dispersion properties in such inhomogeneous plasma is known to enhance the low-frequency noise associated with the Halley's comet [15]. Actually, in space and laboratory plasmas, the equilibrium state is often non-uniform, where the equilibrium quantities vary spatially. Dust density inhomogeneity is known to occur due to the deformation of the Debye sheath [17]. This in turn gives rise to the polarisation force [18], which can make the situation inhomogeneous. Experimental studies of inhomogeneous plasma were done by Ohta and Hamaguchi [19]. Due to these reasons, long back, such inhomogeneous plasma was studied by Nishikawa and Kaw [20]. Very recently, measurement of the amplitude of the dust density wave in inhomogeneous plasma has been reported by Tadsen *et al* [21]. Due to the small fraction of ions, we have considered the dynamics of dust particles in an environment of electrons and positrons only, which are treated to be semiclassical and relativistic. To start with, we have considered the dust density to be homogeneous and applied the usual reductive perturbation technique to deduce the Korteweg–de Vries equation. The corresponding soliton solution properties (amplitude and width) are studied in detail. In the next phase, we have assumed the space variation of the dust density and applied the Krylov–Bogoliubov–Mitropolsky (KBM) method to deduce the variable coefficient nonlinear Schrödinger equation. The modulational stability of this equation is then analysed as a function of plasma parameters and variable density.

In the last section we have demonstrated how an inhomogeneous Korteweg–de Vries equation can be deduced from such a nonlinear Schrödinger equation by Madelung prescription.

2. Formulation

The fluid equation of motion of the plasma can be written as

$$\frac{\partial n_{\mathrm{d}}}{\partial t}+\frac{\partial}{\partial x}(n_{\mathrm{d}}u_{\mathrm{d}})=0, \tag{1}$$

where n_{d} and u_{d} are the dust density and velocity, respectively,

$$\frac{\partial u_{\mathrm{d}}}{\partial t}+u_{\mathrm{d}}\frac{\partial u_{\mathrm{d}}}{\partial x}=\frac{\partial \phi}{\partial x}-\frac{1}{n_{\mathrm{d}}}\frac{\partial P_*}{\partial x}. \tag{2}$$

The force arising due to strong coupling between the dust particles is modelled by an effective electrostatic pressure gradient, where the pressure $P_*=n_{\mathrm{d}}k_{\mathrm{B}}T_*$ with T_* (the effective electrostatic temperature) as defined by Cousens *et al* [6] whose expression is given as

$$T_*=\frac{N_{nn}Z_{\mathrm{d}}^2e^2}{12\pi\epsilon_0 k_{\mathrm{B}}}\sqrt[3]{n_{\mathrm{d}}}(1+\kappa)\exp(-\kappa).$$

Thus, $T_*=T_*(n_{\mathrm{d}},\phi)$ and it is a dynamic quantity with $T_*/T_0=d$ (T_0 is mentioned later in this section). The electrostatic potential is denoted by ϕ.

$$\frac{\partial^2\phi}{\partial x^2}=-\frac{e}{\varepsilon_0}(n_{\mathrm{p}}-n_{\mathrm{e}}-n_{\mathrm{d}}z_{\mathrm{d}}), \tag{3}$$

where electrons and positrons are assumed to obey the density formula of Chandrasekhar [22], expressed as

$$n_{\mathrm{e}}=\frac{8\pi m_{\mathrm{e}}^3c^3}{3h^3}\left[\frac{e^2\phi^2}{m_{\mathrm{e}}^2c^4}+\frac{e\phi}{m_{\mathrm{e}}c^2}\sqrt{(1+n_{\mathrm{e}0}^2)}+n_{\mathrm{e}0}^2\right]^{3/2}, \tag{4}$$

$$n_{\mathrm{p}}=\frac{8\pi m_{\mathrm{p}}^3c^3}{3h^3}\left[\frac{e_{\mathrm{p}}^2\phi^2}{m_{\mathrm{p}}^2c^4}+\frac{e_{\mathrm{p}}\phi}{m_{\mathrm{p}}c^2}\sqrt{(1+n_{\mathrm{p}0}^2)}+n_{\mathrm{p}0}^2\right]^{3/2}. \tag{5}$$

The standard binomial expansion leads to

$$n_{\mathrm{e}}=A_{\mathrm{e}}[\phi^2+\alpha_1\phi+\beta_1], \tag{6}$$

$$n_{\mathrm{p}}=A_{\mathrm{p}}[\phi^2+\alpha_2\phi+\beta_2], \tag{7}$$

$$\left.\begin{aligned}A_{\mathrm{p}}&=\frac{8\pi m_{\mathrm{p}}e_{\mathrm{p}}^2}{3h^3c}\\ \alpha_2&=\frac{3m_{\mathrm{p}}e^2}{e_{\mathrm{p}}}(1+n_{\mathrm{p}0}^2)^{1/2}\\ \beta_2&=n_{\mathrm{p}0}^2\frac{m_{\mathrm{p}}c^2}{e^2}\\ A_{\mathrm{e}}&=\frac{8\pi m_{\mathrm{e}}e^2}{3h^3c}\\ \alpha_1&=\frac{3m_{\mathrm{e}}e}{1}(1+n_{\mathrm{e}0}^2)^{1/2}\\ \beta_1&=n_{\mathrm{e}0}^2\frac{m_{\mathrm{e}}c^2}{e^2}\end{aligned}\right\}. \tag{8}$$

To start with, we consider a homogeneous situation without density gradient. The last two terms on the right-hand side of the momentum equation arise from the

strong coupling force. Final variables of the model are written in terms of dimensionless variables. The number densities are rescaled by their equilibrium values $n = n_{\rm d}/n_{\rm d0}$. We normalise the velocity and potential as follows:

$$\left.\begin{aligned} u &= u_{\rm d}/\sqrt{k_{\rm B}T_0/m_{\rm d}} \\ \phi &= \Phi/(k_{\rm B}T_0/eZ_{\rm d}) \end{aligned}\right\}. \tag{9}$$

The corresponding length is normalised by $\lambda_{\rm D0}$, which is

$$\lambda_{\rm D0} = \sqrt{\frac{\epsilon_0 k_{\rm B} T_0}{n_{\rm d0} e^2 Z_{\rm d}^2}}$$

and the time by $\omega_{\rm d}^{-1}$, the inverse of dust frequency

$$\omega_{\rm d}^{-1} = \sqrt{\frac{\epsilon_0 m_{\rm d}}{n_{\rm d0} e^2 Z_{\rm d}^2}}.$$

Similarly, the electrostatic temperature T_* is normalised by the temperature T_0, where

$$T_0 = \frac{Z_{\rm d}^2 n_{\rm d0} T_{\rm p} T_{\rm e}}{n_{\rm p0} T_{\rm e} + n_{\rm e0} T_{\rm p}}$$

and is written in the dimensionless form in the following equations as d $(= T_*/T_0)$. Next, using eqs (6) and (7) into eq. (3) we get

$$\frac{\partial^2 \phi}{\partial x^2} = (n-1) + c_1\phi + c_2\phi^2 + \cdots. \tag{10}$$

Thus, our set of model equations are as follows:

$$\frac{\partial n_{\rm d}}{\partial t} + \frac{\partial}{\partial x}(n_{\rm d} u_{\rm d}) = 0, \tag{11}$$

$$\frac{\partial u_{\rm d}}{\partial t} + u_{\rm d}\frac{\partial u_{\rm d}}{\partial x} = \frac{\partial \phi}{\partial x} - \frac{\partial d}{\partial x} - n_{\rm d}^{-1} d \frac{\partial n_{\rm d}}{\partial x}, \tag{12}$$

$$\frac{\partial^2 \phi}{\partial x^2} = (n-1) + c_1\phi + c_2\phi^2 + \cdots, \tag{13}$$

where $c_1 = (A_{\rm e} - A_{\rm p})/(n_{\rm d0} Z_{\rm d})$ and $c_2 = (A_{\rm e}\alpha_1 - A_{\rm p}\alpha_2)/(n_{\rm d0} Z_{\rm d})$.

Linearising eqs (11)–(13) by substituting

$$\left.\begin{aligned} n &= 1 + \epsilon n_1 \\ u &= \epsilon u_1 \\ \phi &= \epsilon \phi_1 \\ d &= d_0 + \epsilon d_1 \end{aligned}\right\} \tag{14}$$

and assuming all perturbations to be of the type $\exp[{\rm i}(kx - \omega t)]$, we get the basic dispersion relation

$$k^2 + \frac{(d_{12} - 1)}{\left((\omega^2/k^2) - d_0 - d_{11}\right)} + c_1 = 0, \tag{15}$$

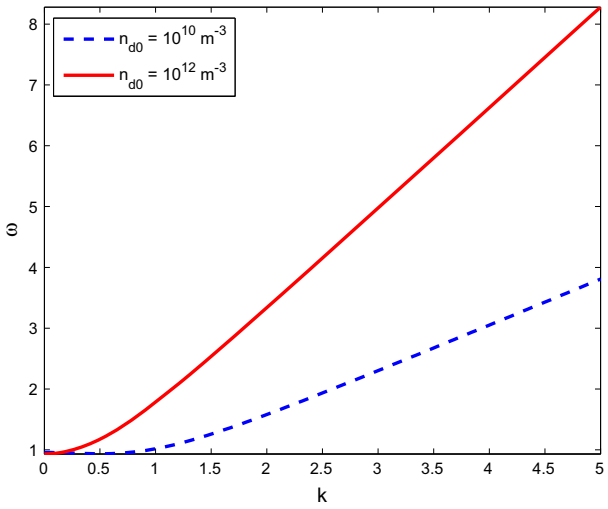

Figure 1. The plot of dispersion relation for various values of dust density. It shows that the slope of ω vs. k curve increases as the dust density ($n_{\rm d0}$) is increased.

where the constants d_0, d_{11} and d_{12} are coefficients obtained due to the perturbative expansion of dimensionless temperature d explained by Cousens *et al* [6] and also given in detail in the appendix of this paper.

A graphical representation of the dispersion relation is given in figure 1, where we have shown variation of ω with k (wave vector), for a specific equilibrium density $n_0 = 1$. Even in figure 1 we can see that there is an influence of the equilibrium dust density ($n_{\rm d0}$) in the dispersion phenomenon. Adapting the usual stretched variables

$$\left.\begin{aligned} \xi &= \epsilon^{1/2}(x - vt) \\ \tau &= \epsilon^{3/2} t \end{aligned}\right\} \tag{16}$$

and expanding the physical quantities as

$$\left.\begin{aligned} u &= \epsilon u_1 + \epsilon^2 u_2 + \epsilon^3 u_3 + \cdots \\ n &= 1 + \epsilon n_1 + \epsilon^2 n_2 + \epsilon^3 n_3 + \cdots \\ \phi &= \epsilon\phi_1 + \epsilon^2\phi_2 + \epsilon^3\phi_3 + \cdots \\ d &= d_0 + \epsilon d_1 + \epsilon^2 d_2 + \epsilon^3 d_3 + \cdots \end{aligned}\right\}. \tag{17}$$

Equating similar powers of ϵ, we get

$$\left.\begin{aligned} u_1 - v n_1 &= 0 \\ -v u_1 &= \phi_1 - d_1 - d_0 n_1 \\ n_1 + \phi_1 &= 0 \end{aligned}\right\}. \tag{18}$$

Hence, from these lowest-order terms we get the phase velocity as

$$v^2 = c_1 + d_0 + d_{11} - d_{12}. \tag{19}$$

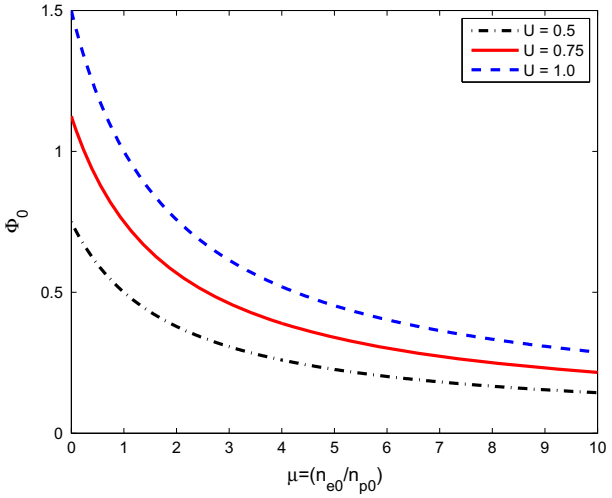

Figure 2. The variation of soliton amplitude (Φ_0) with the electron–position equilibrium density ratio ($\mu = n_{e0}/n_{p0}$). The variations of the amplitude Φ_0 is also observed with the soliton velocity U (in m s^{-1}).

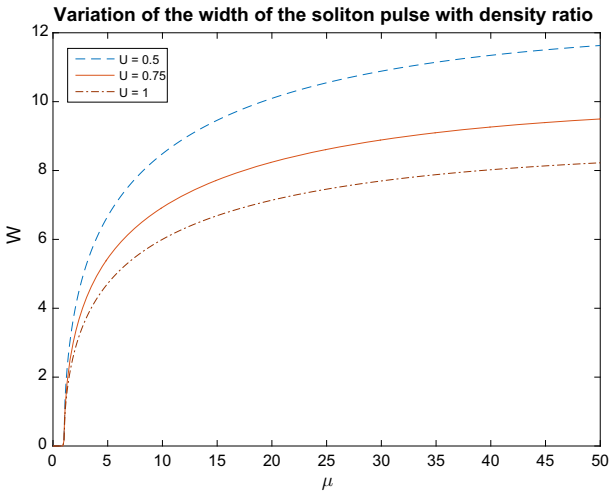

Figure 3. The variation of soliton width (W) with the electron–position equilibrium density ratio ($\mu = n_{e0}/n_{p0}$). The variations of the amplitude Φ_0 is also observed with the soliton velocity U (in m s^{-1}).

Carrying out the computation to higher-order terms, we get Korteweg–de Vries equations:

$$\frac{\partial \phi_1}{\partial \tau} + A\frac{\partial^3 \phi_1}{\partial \xi^3} + B\phi_1 \frac{\partial \phi_1}{\partial \xi}, \tag{20}$$

where

$$A = \frac{v^2 - d_{11} - d_0}{v}, \tag{21}$$

$$B = \frac{1}{v}\{-(3v^2 - 2d_{23} + d_{24} - 2d_{25} + d_{11} - d_{12} - d_0 + 2(v^2 - d_{11} - d_0)c_2)\}. \tag{22}$$

We have omitted the detailed computation, which is very much standardised nowadays. The usual solitary wave solution is

$$\phi_1 = \Phi_0 \operatorname{sech}^2\left(\frac{\xi - U\tau}{W}\right) \tag{23}$$

with

$$\left.\begin{aligned} \Phi_0 &= \frac{3U}{B} \\ W &= 2\sqrt{\frac{A}{U}} \end{aligned}\right\} \tag{24}$$

and U being the velocity of the solitary wave.

A graphical representation of the left-hand side of eq. (15) is given in figure 1, which we refer to as a homogeneous case. The variation of amplitude ϕ_0 for different

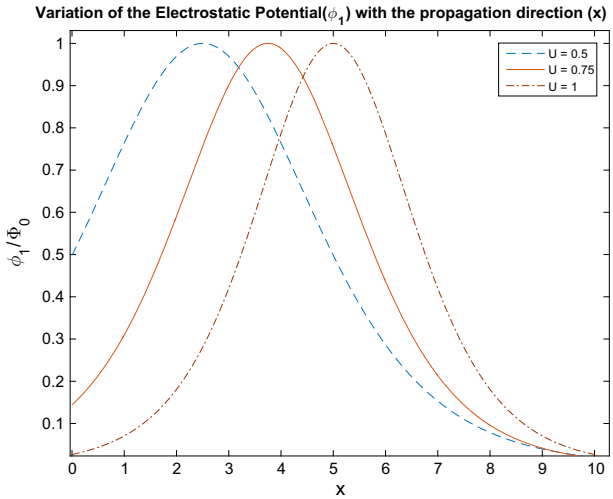

Figure 4. The solution of eq. (23) which shows the shape of the solitary wave profile. We see an amplitude shifting with various values of U (soliton velocity).

values of soliton velocity is shown in figure 2. Here, the independent variable is chosen to be μ ($= n_{e0}/n_{p0}$), the electron–positron density ratio. It is interesting to note that not only μ but also the soliton amplitude varies with the electron–positron temperature. On the other hand, figure 3 shows how the width of the soliton changes with μ. It shows that the width changes significantly with the soliton velocity also.The temperature mentioned in this case is of the order of 10^6 K which is the temperature of plasmas existing in solar corona (as per NRL Plasma Formulary). Figure 4 represents the solution of the Korteweg–de Vries equation (23). It shows the variation of electrostatic potential (ϕ_1) with space. Here we

see that the amplitude of the soliton pulse shifts with the change of soliton velocity U.

3. System with density gradient

To consider a strongly coupled dusty plasma with a density gradient, we have adopted the perturbation method of KBM, which is convenient in the sense that its leads directly to the nonlinear Schrödinger situation, which can always be reduced to the Korteweg–de Vries situation. To start with, we set

$$\left.\begin{aligned} n &= n_0(x) + \epsilon n_1 + \epsilon^2 n_2 + \epsilon^3 n_3 + \cdots \\ u &= \epsilon u_1 + \epsilon^2 u_2 + \epsilon^3 u_3 + \cdots \\ \phi &= \epsilon\phi_1 + \epsilon^2\phi_2 + \epsilon^3\phi_3 + \cdots \\ d &= d_0 + \epsilon d_1 + \epsilon^2 d_2 + \epsilon^3 d_3 + \cdots \end{aligned}\right\}, \tag{25}$$

where each of the dynamical variables n, u, ϕ, etc. are assumed to depend on (x, t) through three variables $a, \bar{a}$ and $\psi = kx - \omega t$ (the phase factor). Here a and $\bar{a}$ denote the complex amplitude of the plane-wave solution of monochromatic emission at zero order. These amplitudes vary slowly as

$$\left.\begin{aligned} \frac{\partial a}{\partial t} &= \epsilon A_1(a, \bar{a}) + \epsilon^2 A_2(a, \bar{a}) + \cdots \\ \frac{\partial a}{\partial x} &= \epsilon B_1(a, \bar{a}) + \epsilon^2 B_2(a, \bar{a}) + \cdots \end{aligned}\right\} \tag{26}$$

together with the complex conjugate of the above relations. Since we regard the medium to be inhomogeneous, we may assume that the undistributed local density is of the zeroth order but its density gradient is of second order, i.e.

$$\frac{\partial n_0}{\partial t} = 0, \quad \frac{\partial n_0}{\partial x} = \epsilon^2\alpha. \tag{27}$$

α is a constant, which is the measure of the density gradient. Substituting in the above equations, we obtain in the lowest order of ϵ:

$$\left.\begin{aligned} u_1 &= a\exp(\mathrm{i}\psi) + \bar{a}\exp(-\mathrm{i}\psi) \\ n_1 &= n_0\frac{k}{\omega}u_1 = n_0\frac{k}{\omega}(a\exp(\mathrm{i}\psi) + \bar{a}\exp(-\mathrm{i}\psi)) \\ \phi_1 &= \beta(a\exp(\mathrm{i}\psi) + \bar{a}\exp(-\mathrm{i}\psi)) \end{aligned}\right\}, \tag{28}$$

where

$$\beta = -\frac{k}{\omega}\frac{\{(\omega^2/k^2) - (d_0 + n_0 d_{11})\}}{(d_{12} - 1)} \tag{29}$$

along with

$$k^2\frac{\partial^2\phi_1}{\partial\psi^2} = n_1 + c_1\phi_1. \tag{30}$$

On combining eqs (25)–(27) we get the dispersion relation in the inhomogeneous case as

$$n_0 + (k^2 + c_1)\left\{\frac{\{(\omega^2/k^2) - (d_0 + n_0 d_{11})\}}{(d_{12} - 1)}\right\} = 0. \tag{31}$$

Equation (31) is the modified form of (16) when there is a density gradient. In our case, we have assumed $n_0(x) = n_{d0}(1 + x/L)$, n_{d0} being the equilibrium density of dust, x is the spatial distance and L is the characteristic length. To study the linear mode of propagation, we have solved (31) and get

$$\omega^2 = \left(\frac{(k^4 + c_1k^2)(n_0d_{11} + d_0) - n_0(d_{12} - 1)}{(k^2 + c_1)}\right). \tag{32}$$

A graphical representation of ω is given in figure 5 where ω's variation with respect to k and x is shown.

Proceeding to the next higher order of ϵ, we get

$$\begin{aligned} &\left\{-k^3\left(\frac{\omega^2}{k^2} - (n_0d_{11} + d_0)\right)\right\}\left[\frac{\partial^3\phi_2}{\partial\psi^3} + \frac{\partial\phi_2}{\partial\psi}\right] \\ &\quad = [A_1 + v_gB_1]\exp(\mathrm{i}\psi) + \mathrm{i}Aa^2\exp(2\mathrm{i}\psi) + \text{c.c.}, \end{aligned} \tag{33}$$

where

$$\begin{aligned} A = \Bigg[&-n_02k\mathrm{i} + \mathrm{i}n_0k - \mathrm{i}k + \frac{n_0k^2}{\omega}\beta\mathrm{i} - 2\mathrm{i}n_0k \\ &\times\left\{d_{23}\left(\frac{n_0k}{\omega}\right)^2 + d_{24}\left(\frac{n_0k}{\omega}\right)\beta + d_{25}\beta^2\right\} \\ &-c_2\left(d_0k + n_0kd_{21} - \frac{\omega^2}{k^2}n_0\right)\beta^2\Bigg], \end{aligned} \tag{34}$$

$$v_g = \frac{\partial\omega}{\partial k} = \frac{(2k^3 + kc_1)(n_0d_{11} + d_0) - \omega^2k}{(c_1 + k^2)}. \tag{35}$$

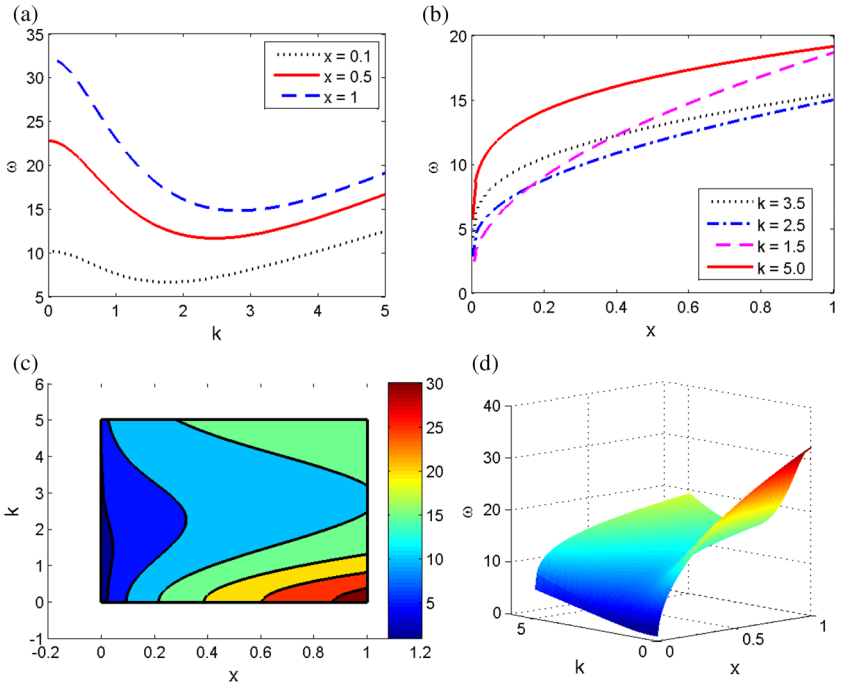

Figure 5. The dispersion relation for inhomogeneous case. The figure clearly shows the change of frequency (ω) with wave vector (k) has a dependence of the space distance x (in m). Parts (**a**) and (**b**) show the variation of ω with the wave vector and spatial distance, respectively while (**c**) and (**d**) give the contour plot and 3D plot of the frequency.

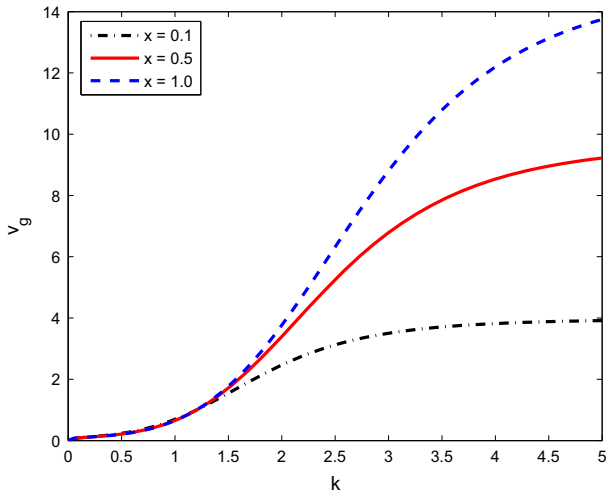

Figure 6. The variation of the group velocity (v_g) with the wave number (k).

V_g is plotted in figure 6. The condition of non-secularity leads to

$$\left.\begin{aligned}\phi_2 &= \alpha_1 a^2 \exp(2\mathrm{i}\psi) + b_1(a,\bar{a})\exp(\mathrm{i}\psi) + \gamma_2(a,\bar{a})\\ n_2 &= \alpha_2 a^2 \exp(2\mathrm{i}\psi) + b_2(a,\bar{a})\exp(\mathrm{i}\psi) + \gamma_3(a,\bar{a})\\ u_2 &= \alpha_3 a^2 \exp(2\mathrm{i}\psi) + b_3(a,\bar{a})\exp(\mathrm{i}\psi) + \gamma_4(a,\bar{a})\end{aligned}\right\} \tag{36}$$

with

$$\begin{aligned}\sigma &= -k^3\left(\frac{\omega^2}{k^2} - (n_0 d_{11} + d_{d_0})\right),\\ \alpha_1 &= \frac{A}{10\sigma},\\ \alpha_2 &= -\alpha_1(1+4k^2) - c_2,\\ \alpha_3 &= \frac{2\mathrm{i}\alpha_2}{k} - \frac{n_0 \mathrm{i}k^2}{\omega},\\ b_2 &= 2\mathrm{i}k\beta - b_1(1+k^2),\end{aligned}$$

which in turn leads to the following equation of ϕ_3:

$$\begin{aligned}\left[\frac{\partial^3\phi_3}{\partial\psi^3} - \frac{\partial\phi_3}{\partial\psi}\right] &= [A_2 + v_g B_2]\exp(\mathrm{i}\psi)\\ &+\mathrm{i}[\omega^2 - k^2(n_0 d_{11} - d_0)]\\ &\times\left(B_1\frac{\partial B_1}{\partial\bar{a}} + \bar{B}_1\frac{\partial B_1}{\partial a}\right)\beta\exp(\mathrm{i}\psi)\\ &+\mathrm{i}\left\{S + k^2 n_0 T + k^2 U_1 + \frac{n_0 k}{\omega}X + \mathrm{i}k^2\alpha_2 V\right\}\\ &\times|a|^2 a\exp(\mathrm{i}\psi) + \mathrm{i}Ya\exp(\mathrm{i}\psi),\end{aligned} \tag{37}$$

where

$$\left.\begin{aligned}
S &= 2k^2n_0 + 2k^2\alpha_3 - 2\frac{k^3}{\omega}n_0\alpha_1 - 2k^2\alpha_2\beta \\
T &= d_{34}\alpha_3 + 2d_{35}\frac{n_0^2}{\omega^2} + \frac{n_0k}{\omega}\beta + d_{37}\frac{n_0k}{\omega}\alpha_1 + d_{39}\beta\alpha_2 \\
U_1 &= \alpha_2 d_{11} + \alpha_1 d_{12} + d_{23}\frac{n_0^2k^2}{\omega^2} + d_{24}\frac{n_0k}{\omega}\beta + d_{25}\beta^2 \\
V &= d_{11}\frac{n_0k}{\omega} + d_{12}\beta + 2k^2\left(d_{11}\frac{n_0k}{\omega} + d_{12}\beta\right) \\
X &= 2\alpha_2 d_{11} + 2d_{12}\alpha_1 + 2\frac{n_0^2k^2}{\omega}d_{23} + 2\beta d_{24} + 2\beta^2 d_{25} \\
Y &= (k^2b_2 + \gamma_3 k) + k^2n_0(d_{11}b_2 + d_{11}\gamma_3) \\
&\quad + k^2n_0(d_{12}b_1 + d_{12}\gamma_2) + k^2(d_{11}b_2 d_{12}\gamma_3) \\
&\quad + k^2(d_{12}b_1 + d_{12}\gamma_2)
\end{aligned}\right\}. \tag{38}$$

If we now demand that all secular terms should vanish, we get

$$[A_2 + v_g B_2] + iP\left(B_1\frac{\partial B_1}{\partial a} + \bar{B}_1\frac{\partial B_1}{\partial \bar{a}}\right) + iQ|a|^2 a + iRa = 0, \tag{39}$$

where

$$\left.\begin{aligned}
P &= ((12k^2 + 2c_1)(n_0d_{11} + d_0) - 2v_g^2k^2 \\
&\quad - 8\omega k v_g - 2\omega^2 - 2c_1v_g^2) \div (2\omega k^2 + 2\omega c_1) \\
Q &= 2n_0k^2 + 2\alpha_3k^2 - \frac{2k^3n_0}{\omega}\alpha_1 - 2k^2\alpha_2\beta \\
&\quad + k^2n_0\left(d_{34}\alpha_3 + 2d_{35}\frac{n_0^2k^2}{\omega^2} + 2\frac{n_0k}{\omega}\beta^2\right. \\
&\quad \left. + \alpha_1 d_{37}\frac{n_0k}{\omega}\beta\alpha_2 d_{39}\right) \\
&\quad + \frac{n_0k}{\omega}\left(2\alpha_2 d_{11} + 2d_{12}\alpha_1 + 2d_{23}\frac{n_0^2k^2}{\omega^2}\right. \\
&\quad \left. + 2\beta d_{24} + \beta^2 d_{25}\right) \\
&\quad + \alpha_2k^2\left(d_{11}\frac{n_0k}{\omega} + \beta d_{12}\right) \\
&\quad + 2k^2\left(d_{11}\frac{n_0k}{\omega} + d_{12}\beta\right) \\
R &= k^2b_2 + k\gamma_3 + k^2n_0(d_{12}b_2 + d_{11}\gamma_3) \\
&\quad + k^2n_0(d_{12}b_1 + d_{12}\gamma_2) \\
&\quad + k^2(d_{11}b_2 d_{11}\gamma_3) + k^2(d_{12}b_1 - d_{12}\gamma_2)
\end{aligned}\right\}. \tag{40}$$

Changing to new variables

$$\left.\begin{aligned}
\tau &= \epsilon^2 t \\
\xi &= \epsilon(x - v_g t)
\end{aligned}\right\} \tag{41}$$

and taking care of the relation

$$\left.\begin{aligned}
A_2 &= \frac{1}{\epsilon^2}\frac{\partial a}{\partial t} - \frac{1}{\epsilon}A_1 \\
B_2 &= \frac{1}{\epsilon^2}\frac{\partial a}{\partial x} - \frac{1}{\epsilon}B_1
\end{aligned}\right\}. \tag{42}$$

We get from eq. (39)

$$i\frac{\partial a}{\partial \tau} + P\frac{\partial^2 a}{\partial \xi^2} + Q|a|^2 a + Ra = 0 \tag{43}$$

which is the nonlinear Schrödinger equation with variable coefficient describing the envelope soliton in the variable density plasma.

4. Modulational instability

In this section we focus on the analysis of the modulational instability of the DAWs in electron–positron–dust plasma as described by the nonlinear Schrödinger equation (43). Modulational instability is a phenomenon whereby deviations from a periodic waveform are reinforced by nonlinearity, leading to the generation of spectral sidebands and the eventual breakup of the waveform into a train of pulses.

To study the modulational instability of eq. (43) we set $a = (a_0 + \delta a(\zeta, \tau))\exp(i\Delta\tau)$, where $\zeta = K\xi - \Omega\tau$, a_0 being the carrier wave amplitude and K and Ω the modulational wave number and frequency respectively.

Using this expression of a in eq. (43), from the zeroth-order term of δa we get

$$\Delta = -Q|a_0|^2 - R.$$

From the first-order term of δa we get

$$i\frac{\partial}{\partial \tau}(\delta a) + \Delta(\delta a) + P\frac{\partial^2}{\partial \xi^2}(\delta a) + Q|a_0|^2(\delta a + \delta a^*) + Q|a_0|^2(\delta a) + R(\delta a) = 0, \tag{44}$$

where δa^* is the complex conjugate of δa. Setting $\delta a = \mathcal{U} + i\mathcal{V}$ and using the expression of Δ obtained from the zeroth-order term of δa, one gets by separating the real and imaginary parts:

$$\left.\begin{aligned}
\frac{\partial \mathcal{U}}{\partial \tau} + P\frac{\partial^2 \mathcal{V}}{\partial \xi^2} &= 0 \\
-\frac{\partial \mathcal{V}}{\partial \tau} + P\frac{\partial^2 \mathcal{U}}{\partial \xi^2} + 2Q\mathcal{U}|a_0|^2 &= 0
\end{aligned}\right\}. \tag{45}$$

Next, assuming plane-wave solutions of $\mathcal{U}$ and $\mathcal{V}$, i.e.

$$\left.\begin{aligned}\mathcal{U} &= \mathcal{S}\exp(\mathrm{i}[K\xi - \Omega\tau])\\ \mathcal{V} &= \mathcal{J}\exp(\mathrm{i}[K\xi - \Omega\tau])\end{aligned}\right\} \tag{46}$$

we arrive at the equation for Ω as

$$\Omega^2 = P^2K^4 - 2PQ|a_0|^2K^2. \tag{47}$$

Equation (47) is referred to as the nonlinear dispersion relation. The stability analysis of Nishikawa and Liu [23] and eq. (47) show that the wave is modulationally stable for $PQ < 0$ and the wave becomes modulationally unstable for $PQ > 0$ provided the modulation wave number K is in the region $0 < K < K_C$, where $K_C = \sqrt{2|Q/P|}|a_0|$ is called the critical wave number. It is also seen that maximum growth rate is obtained for a particular value of modulational wave number $K = K_m = \sqrt{|Q/P|}|a_0|$. Both K_C and K_m are assumed to be less than k.

It is well-known that the modulational instability depends upon the sign of the product of dispersive and nonlinear coefficient, i.e. PQ. Now, as the coefficients P and Q depend on various parameters such as electron–positron density, electron–positron temperature, equilibrium dust density and quite interestingly in this case the spatial distance also, due to which the stability of DAW varies over a wide range of wave number (k). The variation of P and Q is shown in figures 7 and 8, respectively. Figure 7 clearly shows that the dispersive coefficient P eventually changes the sign from positive to negative with the increasing value of wave number (k). Moreover, the figure clearly shows the variation of P with the spatial distance also. Similarly, when the nonlinear coefficient Q is plotted against the wave vector (k), it increases with an increase of the wave vector (k) and always remains positive. But, in this case also, we see that Q also has a prominent dependence on the spatial distance (x). Next, to study the stability condition of the envelope soliton, we have plotted the product of the dispersive and nonlinear coefficient, i.e. PQ against the wave vector (k) represented by figure 9. The figure clearly shows that at first the value of PQ increases with k, remains positive up to a certain value of k and then with further increment of the wave number it becomes negative. Thus, PQ changes sign from positive to negative for a certain range of k. This implies that the PQ also becomes 0 for some value of the wave number (k), which we define as the cut-off value of the wave number. It has been shown earlier also that for cold plasma, in the absence of positron, modulational instability sets in when the modulational wave number $K < K_C = 1.47$ and $PQ > 0$ [24]. But in this case, it is interesting to see that this critical wave number also changes with the spatial distance (x), as shown in figure 10, and its value gets lowered due to the presence of strong coupling. Figure 9 indicates that for $x = 0.1$ the cut-off value is $k \approx 2.35$ while for $x = 0.5$ the cut-off value is $k \approx 2.1$ and for $x = 1.0$ the cut-off value is $k \approx 2.4$.

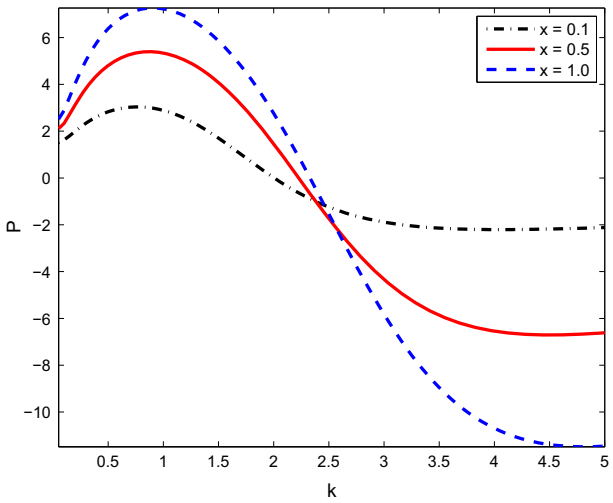

Figure 7. The plot of dispersive coefficient P with wave number (k) which even has a clear variation with the spatial distance (x).

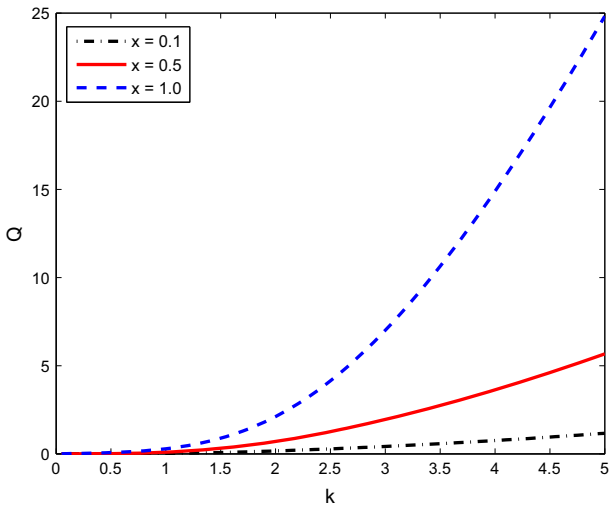

Figure 8. The plot of nonlinear coefficient Q with wave vector (k) which also shows a considerable dependence on the spatial distance (x).

Lastly, we have plotted the instability growth rate, $\Gamma(\mathrm{Im}(\Omega))$ in figure 11. We can see that the instability growth rate also varies with the spatial distance (x).

In this connection, one may note that if we make a change of variable $a = b\exp(\mathrm{i}R\tau)$ in eq. (43), we get the standard form of nonlinear Schrödinger equation:

$$\mathrm{i}\frac{\partial b}{\partial \tau} + P\frac{\partial^2 b}{\partial \xi^2} + Q\,|b|^2\,b = 0. \tag{48}$$

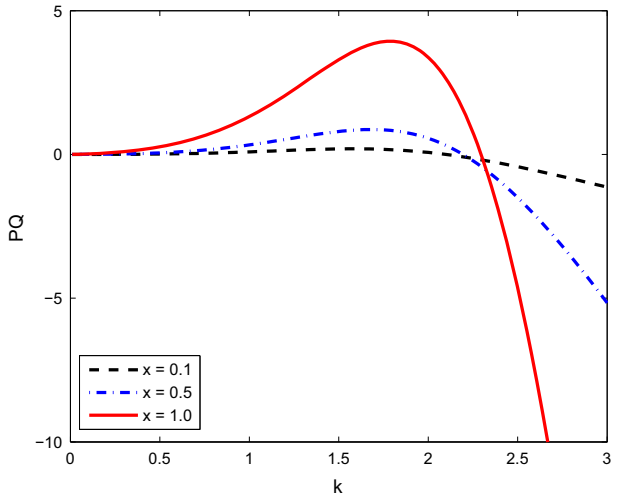

Figure 9. The plot of the product of nonlinear and dispersive coefficient PQ for various values of spatial distance with wave vector (k).

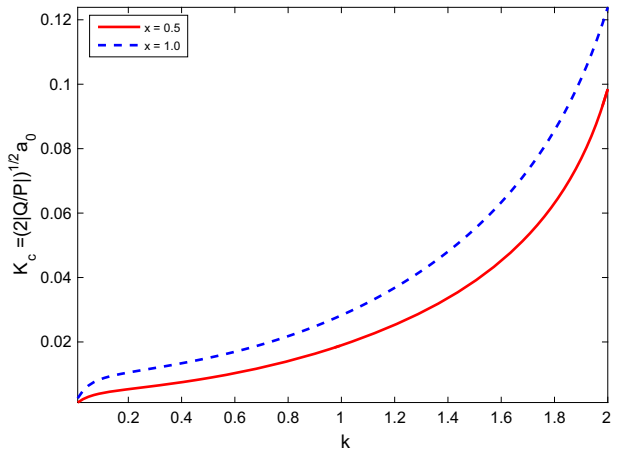

Figure 10. The variation of the critical wave number (K_C), which is the maximum value of the modulational wave number up to which the wave is unstable for $PQ > 0$.

5. Madelung connection

In the first part of our analysis, we have shown how Korteweg–de Vries equation describes the excitation of the nonlinear wave in the uniform density case. On the other hand, in the second part with density gradient, we have adopted the KBM approach and obtained the variable coefficient nonlinear Schrödinger equation, stability of which is analysed. The connection between Korteweg–de Vries and nonlinear Schrödinger equations was explored long ago in an elegant way by Madelung using the fluid dynamic formulation [25]. Here we show how this variable coefficient nonlinear Schrödinger equation can also be connected in a similar manner.

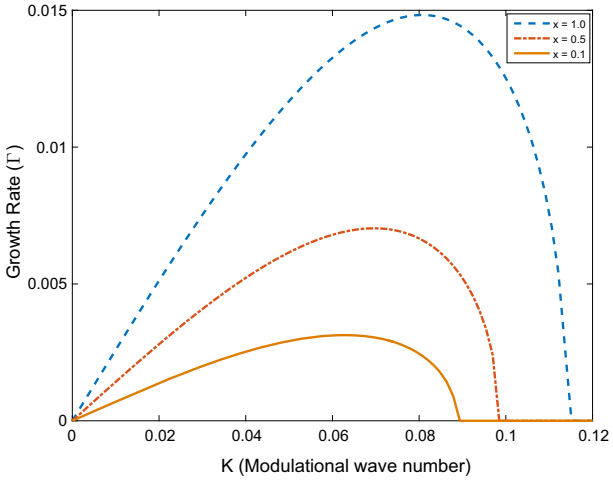

Figure 11. The plot of growth rate of instability (Γ) of the wave.

To illustrate the equation, we consider the nonlinear Schrödinger equation (44). We substitute $b = \sqrt{\rho}\exp(\mathrm{i}\theta)$ in eq. (44) and separating the real and imaginary parts, we get the generalised Madelung equation as

$$P'\rho\left(\frac{\partial}{\partial\tau}+\mathcal{W}\frac{\partial}{\partial\xi}\right)\mathcal{W} = -\mathcal{W}\frac{\partial\rho}{\partial\tau} - \mathcal{W}^2P'\frac{\partial\rho}{\partial\xi} + P'\rho\frac{\partial\mathcal{W}}{\partial\rho}, \tag{49}$$

where $\mathcal{W} = \theta_\xi$.

The other one is

$$\rho\frac{\partial\mathcal{W}}{\partial\tau} + P\frac{\partial}{\partial\xi}[P'\mathcal{W}^2] = 2\rho\frac{\partial}{\partial x}[Q\mathcal{W}] + \rho\frac{\partial}{\partial\xi}\left\{P'\left(\frac{\rho^{-1}}{2}\rho_{xx} - \frac{\rho^{-2}}{4}\rho_x^2\right)\right\}. \tag{50}$$

At this point, one should note that

$$\frac{\partial}{\partial x}\left(\frac{1}{\rho^{1/2}}\frac{\partial^2\rho^{1/2}}{\partial x^2}\right) = \frac{\partial}{\partial x}\left(\frac{\rho^{-1}}{2}\rho_{xx} - \frac{\rho^{-2}}{4}\rho_x^2\right) = \frac{1}{\rho}\left(\frac{1}{2}\frac{\partial^3\rho}{\partial x^3} - 4\frac{\partial\rho^{1/2}}{\partial x}\frac{\partial^2\rho^{1/2}}{\partial x^2}\right). \tag{51}$$

Equations (45) and (46) are the two generalised Madelung forms derived from the variable coefficient nonlinear Schrödinger equation, which can be simply solved if P and Q are constants and some assumptions are made about $\mathcal{W} = \partial\theta/\partial\xi$ depending upon the boundary condition.

6. Conclusion and discussion

In our analysis, we have considered a semiclassical relativistic dusty plasma with a density gradient due to its importance in astrophysical situations in the strong coupling regime. The ions and the electrons are assumed to behave as per Chandrasekhar's equations [26]. In the first part of our computation, we have assumed a uniform density situation and have used the reductive perturbation technique to deduce the Korteweg–de Vries equation. The amplitude and width of the corresponding solitary wave are computed and its variations are studied with respect to μ $(= n_{e0}/n_{p0})$. The parameter values considered for the computations carried out in this paper are $n_{e0} = 7 \times 10^{23}\,\mathrm{m}^{-3}$, $n_{p0} = 3 \times 10^{23}\,\mathrm{m}^{-3}$ and $n_{d0} \sim 10^{18}\,\mathrm{m}^{-3}$ and the temperatures of electrons and positrons are taken to be $T_e = 5 \times 10^6$ K and $T_p = 10^6$ K, which are found in different astrophysical environments and in laboratory laser plasmas [27].

In the second half, we have considered the situation with density gradient and used the KBM method to deduce a nonlinear Schrödinger equation with variable coefficient. In fact, in the homogeneous situation, we see that the wave frequency ω is monotonically increasing with wave vector (k), but when the situation is inhomogeneous, the variation of ω is seen to have a spatial dependence. Moreover, at first, with the increase of k, the wave frequency shows a decreasing trend, but after a certain value of k, it goes on increasing. A detailed study has been performed on the modulational stability of eq. (43), which reveals a new type of behaviour due to the spatial dependence of the dispersive and nonlinear coefficients (i.e. P and Q, respectively) coming from the spatial variation of the equilibrium dust density. This leads to a change in the behaviour of P with respect to the spatial distance, as seen in figure 7 and by Q, as shown in figure 8. Next, in the modulational stability section, we analysed the stability condition of the envelope soliton, which implies the formation of dark or bright envelopes through the sign of the product of dispersive and nonlinear coefficient, i.e. PQ which is shown in figure 9. Moreover, as PQ changes from positive to negative, we get a cut-off value of k, i.e. the value of k for which PQ becomes 0. If we take a close look at figure 9, it can be seen that this cut-off value of k also varies with spatial distance. Further, as we have seen in §4, the critical wave number (K_C) depends upon the coefficients P and Q and evidently varies with spatial distance (x), which is shown in figure 10.

Lastly, in an attempt to connect this new nonlinear Schrödinger equation with the previous Korteweg–de Vries problem, we have taken recourse to the Madelung-type transformation. This mapping actually leads to a new form of Korteweg–de Vries equation with variable coefficients.

Appendix A.

To deduce the expression for the expansion coefficients of d (we have used up to d_3), we start with the definition of the Debye length:

$$\begin{aligned}\frac{\lambda_D}{\lambda_{D0}} &= \sqrt{\left(\frac{n_{i0}T_e + n_{e0}T_i}{n_i T_e + n_e T_i}\right)} \\ &= \left\{\frac{1+\mu\theta}{\exp(-(1-\mu)/(1+\mu\theta)\phi) + \mu\theta\exp\left((1-\mu)\theta/(1+\mu\theta)\phi\right)}\right\}^{1/2} \\ &= \frac{1}{\left[\sum_{j=0}^{n}(j+1)c_{j+1}\phi^j\right]^{1/2}}. \end{aligned} \tag{A1}$$

On the other hand,

$$\begin{aligned}\mathcal{K} &= \frac{1}{\lambda_D n_d^{1/3}} \\ &= \frac{1}{\lambda_{D0} n_d^{1/3}}\left[\sum_{j=0}^{\infty}(j+1)c_{j+1}\phi^j\right]^{1/2} \\ &= \frac{1}{\lambda_{D0}}\left[1 + 2c_2\phi + 3c_3\phi^2 + 4c_4\phi^3 + \cdots\right]^{1/2} \\ &\quad \times n_{d0}\left\{1 + \epsilon n_1 + \epsilon^2 n_2 + \epsilon^3 n_3 + \cdots\right\}^{1/3}. \end{aligned} \tag{A2}$$

Hence, if we set

$$\mathcal{K} = \mathcal{K}_0 + \epsilon\mathcal{K}_1 + \epsilon^2\mathcal{K}_2 + \epsilon^3\mathcal{K}_3 + \cdots,$$

then

$$\begin{aligned}\mathcal{K}_1 &= -\frac{1}{3}n_1 + c_2\phi_1, \\ \mathcal{K}_2 &= -\frac{1}{3}n_2 - \frac{1}{3}c_2 n_1\phi_1 + \frac{3c_3}{2}\phi^2 \\ &\quad + \frac{c_2^2\phi_1^2}{2} + c_2\phi_2 + \frac{2}{9}n_1^2,\end{aligned}$$

$$\mathcal{K}_3 = -\frac{n_3}{3} + c_2\phi_3 - \frac{c_2}{3}(n_2\phi_1 + n_1\phi_2) + \frac{2}{9}c_2\phi_1 n_1^2 - \left(\frac{3c_3 - c_2^2}{6}\right) n_1\phi_1^2. \tag{A3}$$

Let us recapitulate T_*,

$$T_* = \frac{N_{nn}Z_{\mathrm{d}}^2 e^2}{12\pi\epsilon_0 k_{\mathrm{B}}}\sqrt[3]{n_{\mathrm{d}}}(1+\mathcal{K})\exp(-\mathcal{K}),$$

so that

$$\begin{aligned} d = {} & \frac{N_{nn}Z_{\mathrm{d}}^2 e^2}{12\pi\epsilon_0 k_{\mathrm{B}}}\sqrt[3]{n_{\mathrm{d}0}}(1+\mathcal{K}_0)\exp(-\mathcal{K}_0) \\ & \times \left(1 + \epsilon n_1 + \epsilon^2 n_2 + \epsilon^3 n_3 + \cdots\right)^{1/3} \\ & \times \left(1 + \epsilon\frac{\mathcal{K}_1}{1+\mathcal{K}_0} + \epsilon^2\frac{\mathcal{K}_2}{1+\mathcal{K}_0} + \epsilon^3\frac{\mathcal{K}_3}{1+\mathcal{K}_0} + \ldots\right) \\ & \times \left\{1 - \left(\epsilon\mathcal{K}_1 + \epsilon^2\mathcal{K}_2 + \epsilon^3\mathcal{K}_3\right) - \frac{1}{2}\left(\epsilon\mathcal{K}_1 + \epsilon^2\mathcal{K}_2 + \epsilon^3\mathcal{K}_3\right)^2 + \ldots\right\}. \end{aligned} \tag{A4}$$

On comparing the coefficients of ϵ we can get

$$\left.\begin{aligned} d_1 &= d_{11}n_1 + d_{12}n_2 \\ d_2 &= d_{21}n_2 + d_{22}\phi_2 + d_{23}n_1^2 + d_{24}n_1\phi_1 d_{25}\phi_1^2 \end{aligned}\right\} \tag{A5}$$

$$\left.\begin{aligned} d_{11} = d_{21} &= \frac{d_0}{3}\frac{\mathcal{K}_0}{1+\mathcal{K}_0} \\ d_{12} = d_{22} &= -c_2 d_0\frac{1}{1+\mathcal{K}_0} \\ d_{23} &= \frac{d_0}{18}\frac{\mathcal{K}_0 - 1}{\mathcal{K}_0 + 1} \\ d_{24} &= -\frac{d_0}{3}c_2\frac{2\mathcal{K}_0 + 3}{1+\mathcal{K}_0} \\ d_{25} &= \frac{d_0}{3}\left(\frac{3c_3 - c_2^2\mathcal{K}_0}{1+\mathcal{K}_0}\right) \end{aligned}\right\} \tag{A6}$$

$$\begin{aligned} d_3 = {} & d_{31}n_3 + d_{32}\phi_3 + d_{33}n_1^3 + d_{34}n_1 n_2 + d_{35}n_1^2\phi_1 \\ & + d_{36}n_1\phi_1^2 + d_{37}n_1\phi_2 + d_{38}n_1\phi_2^2 + d_{39}n_2\phi_1 \\ & + d_{310}\phi_1^3 + d_{311}\phi_1^2 + d_{312}\phi_1\phi_2^2, \end{aligned} \tag{A7}$$

where

$$\left.\begin{aligned} d_{31} &= \frac{d_0}{3}\frac{\mathcal{K}_0}{1+\mathcal{K}_0} \\ d_{32} &= -c_2 d_0\frac{1}{1+\mathcal{K}_0} \\ d_{33} &= \frac{25\mathcal{K}_0 + 31}{81(1+\mathcal{K}_0)}d_0 \\ d_{34} &= -\frac{\mathcal{K}_0 + 2}{9(1+\mathcal{K}_0)}d_0, \\ d_{35} &= \left[\frac{c_2}{9} - \frac{c_2}{9}\frac{1}{\mathcal{K}_0 + 1}\right]d_0 \\ d_{36} &= \left[-c_3 - \frac{c_2^2}{3(1+\mathcal{K}_0)}\right]d_0 \\ d_{37} &= -\frac{c_2}{3}d_0, \quad d_{38} = \frac{c_2}{3}\frac{1}{\mathcal{K}_0 + 1}d_0 \\ d_{39} &= \left[-\frac{c_2}{3} + \frac{c_2}{3(1+\mathcal{K}_0)}\right]d_0 \\ d_{310} &= \left[-\frac{c_2}{3} - \frac{(3c_3 - c_2^2)c_2}{(1+\mathcal{K}_0)^2}\right]d_0 \\ d_{311} &= c_2 d_0 \\ d_{312} &= c_2^2\frac{1}{1+\mathcal{K}_0}d_0 \end{aligned}\right\}. \tag{A8}$$

References

[1] H R Prabhakara and V L Tanna, *Phys. Plasmas* **3(8)**, 3176 (1996)
[2] M Eghbali and B Farokhi, *Pramana – J. Phys.* **84(4)**, 637 (2015)
[3] G Gozadinos, A V Ivlev and J P Boeuf, *New J. Phys.* **5(1)**, 32 (2003)
[4] R X Luo, H Chen and S Q Liu, *IEEE Trans. Plasma Sci.* **43(6)**, 1845 (2015)
[5] M G M Anowar, M S Rahman and A A Mamun, *Phys. Plasmas* **16(5)**, 053704 (2009)
[6] S E Cousens, S Sultana, I Kourakis, V V Yaroshenko, F Verheest and M A Hellberg, *Phys. Rev. E* **86**, 066404 (2012)
[7] R Lallement, B Y Welsh, M A Barstow and S L Casewell, *Astron. Astrophys.* **533**, A140 (2011)
[8] A Rahman, S Ali, A M Mirza and A Qamar, *Phys. Plasmas* **20(4)**, 042305 (2013)
[9] M Masum Haider *et al*, *Open Phys.* **10**, 1168 (2012)
[10] H Ikezi, *Phys. Fluids* **29(6)**, 1764 (1986)
[11] B M Veeresha, S K Tiwari, A Sen, P K Kaw and A Das, *Phys. Rev. E* **81**, 036407 (2010)
[12] N N Rao, P K Shukla and M Y Yu, *Planet. Space Sci.* **38(4)**, 543 (1990)
[13] P K Shukla and V P Silin, *Phys. Scr.* **45(5)**, 508 (1992)

[14] A Barkan, R L Merlino and N D'angelo, *Phys. Plasmas* **2(10)**, 3563 (1995)
[15] S Singh and R Bharuthram, *IEEE Trans. Plasma Sci.* **38(4)**, 852 (2010)
[16] S A El-Wakil, M A Zahran, E K El-Shewy and A E Mowafy, *Phys. Scr.* **74(5)**, 503 (2006)
[17] K E Lonngren and I Alexeff, *Phys. Plasmas* **15(9)**, 093505 (2008)
[18] M Asaduzzaman and A A Mamun, *Phys. Plasmas* **19(9)**, 093704 (2012)
[19] H Ohta and S Hamaguchi, *Phys. Rev. Lett.* **84(26)**, 6026 (2000)
[20] K Nishikawa and P K Kaw, *Phys. Lett. A* **50(6)**, 455 (1975)
[21] B Tadsen, F Greiner and A Piel, *Phys. Plasmas* **24(3)**, 033704 (2017)
[22] S Chandrasekhar, *An introduction to the study of stellar structure*, Astrophysical monographs (Dover Publications, New York, 1957)
[23] K Nishikawa and C S Liu, *Adv. Plasma Phys.* **6**, 1 (1976)
[24] J K Chawla, M K Mishra and R S Tiwari, *Astrophys. Space Sci.* **347(2)**, 283 (2013)
[25] R Fedele and H Schamel, *Eur. Phys. J. B* **27(3)**, 313 (2002)
[26] S Chandrasekhar, *Mon. Not. R. Astron. Soc.* **95**, 207 (1935)
[27] D Chatterjee and A P Misra, *Phys. Plasmas* **23(10)**, 102114 (2016)